

# Advanced Modeling and Uncertainty Quantification for Flight Dynamics; Interim Results and Challenges

David C. Hyde<sup>1</sup>, Kamal M. Shweyk<sup>2</sup>, and Frank Brown<sup>3</sup>  
*Boeing Research & Technology, Huntington Beach, CA, 92646*

*and*

Gautam Shah<sup>4</sup>  
*NASA Langley Research Center, Hampton VA 23681*

As part of the NASA Vehicle Systems Safety Technologies (VSST), Assuring Safe and Effective Aircraft Control Under Hazardous Conditions (Technical Challenge #3), an effort is underway within Boeing Research and Technology (BR&T) to address Advanced Modeling and Uncertainty Quantification for Flight Dynamics (VSST1-7). The scope of the effort is to develop and evaluate advanced multidisciplinary flight dynamics modeling techniques, including integrated uncertainties, to facilitate higher fidelity response characterization of current and future aircraft configurations approaching and during loss-of-control conditions. This approach is to incorporate multiple flight dynamics modeling methods for aerodynamics, structures, and propulsion, including experimental, computational, and analytical. Also to be included are techniques for data integration and uncertainty characterization and quantification. This research shall introduce new and updated multidisciplinary modeling and simulation technologies designed to improve the ability to characterize airplane response in off-nominal flight conditions. The research shall also introduce new techniques for uncertainty modeling that will provide a unified database model comprised of multiple sources, as well as an uncertainty bounds database for each data source such that a full vehicle uncertainty analysis is possible even when approaching or beyond Loss of Control boundaries. Methodologies developed as part of this research shall be instrumental in predicting and mitigating loss of control precursors and events directly linked to causal and contributing factors, such as stall, failures, damage, or icing. The tasks will include utilizing the BR&T Water Tunnel to collect static and dynamic data to be compared to the GTM extended WT database, characterizing flight dynamics in off-nominal conditions, developing tools for structural load estimation under dynamic conditions, devising methods for integrating various modeling elements into a real-time simulation capability, generating techniques for uncertainty modeling that draw data from multiple modeling sources, and providing a unified database model that includes nominal plus increments for each flight condition. This paper presents status of testing in the BR&T water tunnel and analysis of the resulting data and efforts to characterize these data using alternative modeling methods. Program challenges and issues are also presented.

---

<sup>1</sup> Technical Fellow, Boeing Research & Technology, 5301 Bolsa Ave M/S H017-D334, AIAA Associate Fellow.

<sup>2</sup> Manager, Boeing Research & Technology, 5301 Bolsa Ave M/S H017-D334, AIAA Associate Fellow.

<sup>3</sup> Aerospace Engineer, Boeing Research & Technology, 5301 Bolsa Ave M/S H017-D334, AIAA Member.

<sup>4</sup> Assistant Head, Flight Dynamics Branch, MS308, AIAA Senior Member

## NOMENCLATURE

$\alpha$ , AOA	angle of attack, deg.
$\beta$ , beta	angle of sideslip, deg
BR&T	Boeing Research and Technology
CD	drag coefficient
CL	lift coefficient
CL <sub>max</sub>	maximum lift coefficient
Cl	body axis rolling moment coefficient
Cl <sub>p</sub>	body axis roll rate damping derivative, 1/rad
Cl <sub>q</sub>	body axis rolling moment due to pitch rate, 1/rad.
Cl <sub>r</sub>	body axis rolling moment due to yaw rate, 1/rad.
Cm	pitching moment
Cm <sub>p</sub>	pitching moment due to roll rate, 1/rad.
Cm <sub>q</sub>	pitch rate damping derivative, 1/rad
Cm <sub>r</sub>	pitching moment due to yaw rate, 1/rad.
Cn	body axis yawing moment coefficient
Cn <sub>p</sub>	body axis yawing moment due to roll rate, 1/rad.
Cn <sub>q</sub>	body axis yawing moment due to pitch rate, 1/rad
Cn <sub>r</sub>	body axis yaw rate damping derivative, 1/rad.
CY	side force coefficient
DOF	Degree of Freedom
FVWT	Flow Visualization Water Tunnel
GTM	Generic Transport Model
k	Strouhal number (reduced frequency), $\frac{\omega l}{2V}$
l	Characteristic length; (b or $\bar{c}$ )
LOC	Loss of Control
NAART	North American Aviation Research Tunnel
p	body axes roll rate, rad/sec
$\hat{p}$	non-dimensional roll rate (reduced), $\frac{pb}{2V}$ , rad
q	pitch rate, rad/sec
$\hat{q}$	non-dimensional pitch rate (reduced), $\frac{q\bar{c}}{2V}$ , rad
r	body axes yaw rate, rad/sec
$\hat{r}$	non-dimensional yaw rate (reduced), $\frac{rb}{2V}$ , rad
SPM	Single Point Method
$\omega$	oscillation frequency; $\frac{p_{\max}}{\text{Amplitude}}$ , 1/sec
VSST	Vehicle System Safety Technologies

## **INTRODUCTION**

### **BACKGROUND**

Reducing Loss of Control (LOC) events on commercial transport aircraft is one of the Technical Challenges of the VSST project at NASA. Characterization of the dynamic and unsteady behavior of aircraft during these events is a cornerstone of the project. As part of the VSST research, BR&T is duplicating and expanding NASA's extensive GTM dynamic derivative database using proven methods, tools, and facilities such as the Boeing Research & Technology (BR&T) Flow Visualization Water Tunnel (FVWT). The research will include developing, demonstrating, and documenting new methods of analysis and integration to determine expanded parameters of interest for characterization of steady and unsteady aerodynamic effects using experimental data.

### **PURPOSE**

This research will introduce new and updated multidisciplinary modeling and simulation technologies that will improve NASA's ability to characterize airplane response in off-nominal flight conditions that precede and carry through LOC. The program will also introduce new techniques for uncertainty modeling that will provide a unified database model comprised of multiple sources, as well as an uncertainty bounds database for each data source such that a full-vehicle uncertainty analysis is possible even when approaching or beyond LOC boundaries. Methodologies developed as part of this research will be instrumental in predicting and mitigating loss of control precursors and events directly linked to causal and contributing factors, such as stall, failures, damage, or icing. Further, the flexibility of these methodologies will ensure they are applicable to sequential precursors such that the entire event chain from initial precursor to accident or recovery can be replicated and eventually predicted and, thus, mitigated. The proposed work for Assuring Safe and Effective Aircraft Control under Hazardous Conditions Technical Challenge (VSST TC-3) will improve the predictive capability for modeling tools and methods in order to reduce the likelihood of LOC events.

The goal is to develop multi-disciplinary system modeling solutions able to predict and replicate, and thus mitigate, sequentially occurring hazards that increase the likelihood of LOC events. Specific research objectives include the development, evaluation, and validation of modeling tools and methods that include:

- a) Methods for characterizing the dynamic response of a vehicle in off-nominal conditions due to steady and unsteady aerodynamic effects, propulsive effects, and aero-structural effects;
- b) Tools for structural load estimation under dynamic conditions that can be used to estimate vehicle maneuvering limitations;
- c) Development of model-validation experiments to measure the predictive capability of experimental and computationally-derived models;

- d) Methods for integration of various modeling elements (e.g., aero, structures, propulsion, etc.) into a real-time simulation modeling capability;
- e) Data fusion techniques to merge multi-source data into a unified aerodynamic database including uncertainty;
- f) Development of techniques to generate uncertainty models using real-time system identification data;
- g) Uncertainty modeling techniques able to capture both aleatory and epistemic uncertainties; and
- h) Tools and methods for propagating uncertainties in the aerodynamic database to give bounds on vehicle system response predictions.

This paper focuses on item (a); specifically the static and forced-oscillation testing in the Boeing FVWT and the data reduction of same, and the dynamic modeling techniques developed, analyzed, and assessed using these data.

## **DESCRIPTION OF TEST FACILITIES**

### **BOEING FLOW VISUALIZATION WATER TUNNEL**

In August 1990, Rockwell International took delivery of a Water Tunnel (Model 2436) from Eidetic Corporation, whose water tunnel manufacturing and research operations were spun off into Rolling Hills Research Corporation in 2002. In December 1996, the Boeing Company acquired the defense and aerospace business of Rockwell International, including what was once North American Aviation, and, in the process, inherited the Water Tunnel. As a result of this acquisition, Boeing also took possession of a co-located, low-speed, wind tunnel, namely the North American Aviation Research Tunnel (NAART), built by Aerolabs, as well as a dedicated machine shop.

As delivered, the Water Tunnel consisted of a C-strut support system with a turntable that provided pitch and yaw control, and came equipped with six colored dye containers for flow visualization. The closed-system, horizontal configuration of the Water Tunnel, pictured in Figure 1, allows easy access to the model through the open top of the test section, which is 24 in. wide by 26 in. high by 72 in. long, with tempered glass panels on all three other sides to permit multiple viewing and recording angles. The maximum speed of the water is 1 ft/sec resulting in a Reynold's no. of under 100,000/ft.

In 2004 the FVWT was fitted with a 6 degree of freedom (DOF) motion rig with dynamic force and moment measurement capabilities. In a sub-scale wind tunnel, dynamic rates are higher than full scale rates. In a water tunnel, reduced scale and fluid velocity results in scaled dynamic motions that are slower than full scale and sub-scale dynamic-balance wind tunnels. This yields easier motion control and data capture, better flow visualization, negligible inertial tares, and negligible dynamic interactions with model, hence avoiding the need for high support stiffness.

## **BALANCE**

The FVWT has a submersible, 6 DOF, fully automated, computer controlled balance with static and dynamic testing capabilities. The balance hardware and control software combined are called Scorpio produced by AeroArts of Torrance, CA. The upper structure, visible in Figure 1, is approximately seven feet high and consists of six vertical linear actuators. Below the upper structure is a box containing the body-axis roll motor that is connected to the actuators via carbon fiber struts. The model is mounted in front of the roll box, as illustrated in Figure 1. The six vertical actuators and roll box together maneuver the model through the commanded motions. Between the roll motor and the model is an adjustable pitch arc that is capable of initial position offsets between -60 to 60 deg AOA.

## **GENERIC TRANSPORT MODEL**

The FVWT test model was a 14% scale<sup>1</sup> model of the NASA Generic Transport Model (GTM). A 3-view of the model is presented in Figure 2. The GTM is a 5.5% -scale version of a generic twin-engine, commercial transport aircraft. The test model was made using a fused deposition modeling technique to create each part layer by layer with a continuous strip of ABS plastic filament. The processes used a Fortus<sup>®</sup> 3D printer guided by a CAD geometry file. Some minor hand finishing work was required to smooth the parts prior to testing.

The NASA GTM aero database and GTM Simulation aerodynamic model are based on a dynamically scaled GTM. This model was treated as the reference basis for the FVWT test and all data comparisons presented in this report.

## **SCOPE**

The FVWT test consisted of static force and moment testing and dynamic forced-oscillation testing. Dynamic runs included pitch, roll, and yaw constant frequency oscillations at multiple frequencies and amplitudes selected to align with existing NASA GTM data. Constant-amplitude, increasing-frequency sweeps were conducted in all axes for equivalent systems analyses, and large-amplitude low-rate sweeps were conducted in pitch and yaw to evaluate aerodynamic hysteresis effects. Model components with deflected control surfaces were constructed; however, due to time constraints the model was tested in the FVWT with all surfaces in a faired-condition only.

## **METHOD OF TEST**

### **STATIC TESTING**

The objectives of the static force and moment test runs for the FVWT Test were to establish a comparison between the FVWT data and the NASA 14x22 wind tunnel data and demonstrate repeatability of the FVWT data from similar runs conducted separately. Other research topics of

---

<sup>1</sup> The 14% scale is relative to the NASA 'AirSTAR' scaled GTM

interest were the effects of sweep rate, flow angularity, model symmetry, and the influence of model orientation. Pitch-pause and pitch sweep runs were conducted at similar conditions to investigate the effect of sweep rate. During a pitch sweep, the model was continuously swept from the lowest AOA in the schedule to the highest at a constant angular rate. For a pitch-pause run, the model paused at each commanded AOA, typically every 2 degrees, for a period of time, typically 50 seconds. The pitch sweeps were conducted at 0 deg beta and -16 to 30 deg AOA. One pitch sweep was completed with the model inverted (180 deg phi), to investigate the influence of model orientation on these data and determine flow angularity. The pitch-pause runs were performed from -4 to 28 deg AOA, with pauses at every 2 deg AOA. Pitch-pause runs were completed for 0, -4, and 4 deg beta, to check model symmetry. Yaw-pause runs were completed at 0, 5, 10, and 15 deg AOA for -20 to 20 deg beta. Yaw sweeps were run in both directions at 10 deg AOA at a constant rate from -20 to 20 deg beta. One yaw sweep was run with the model rolled 90 deg.

## **DYNAMIC TESTING**

### **Constant Frequency Oscillations**

Pitch, roll, and yaw oscillation runs were developed to estimate dynamic derivatives. Each series in the matrix consisted of 12 oscillatory runs varying from -4 deg AOA to 26 deg AOA. At each AOA, 10 oscillations were completed at a constant oscillatory frequency. The frequencies were selected to match available GTM data from prior NASA testing.

### **Frequency Sweeps**

Frequency sweeps were conducted in three axes, pitch, roll, and yaw at 5, 15, 25, 35, and 45 deg AOA. The sweep runs commanded constant amplitude, increasing frequency oscillations. A tool was developed by BR&T to determine the desired sweep frequency and amplitude prior to testing. Constant rate (varying amplitude) frequency sweeps were also planned, but not completed due to time constraints.

### **Hysteresis Sweeps**

Pitch and yaw hysteresis runs commanding large amplitude oscillations at 0.4 deg/sec were completed. The pitch hysteresis runs were designed to reach CLmax, 5 deg less than CLmax, 10 deg less than CLmax, and 15 deg less than CLmax. The yaw hysteresis runs swept from -25 to 25 deg beta at approximately 0.4 deg/sec.

## **RESULTS AND DISCUSSION**

### **STATIC FORCE AND MOMENT TESTING**

The static portion of FVWT testing included 15 runs focused on providing a foundation for the oscillatory test matrix and data reduction as well as facilitating comparisons with NASA wind tunnel data. In a typical force and moment wind tunnel test the coefficient values measured at each angle of attack would be averaged over the time of collection and only the average value would be preserved for analysis. In the case of this test, however, the time-history data were

preserved at the raw collection rate of 40 Hz to better assess the quality of the data to evaluate unsteady and/or nonlinear effects. All of the reduced data presented in this report show the mean coefficient values. The time history data are preserved in run files managed separately.

### **FORCE AND MOMENT DATA REPATABILITY**

Force and moment repeatability was evaluated by comparing identical-condition sequential pitch pause runs. Run repeatability results are presented for longitudinal and lateral-directional coefficients in Figures 3 and 4 respectively. Lift coefficient repeatability was within 10% relative error for AOA > 10 deg. Pitching moment repeatability was very good at AOAs below 9 deg and within 10% relative error for AOA > 9 deg. In that standard repeatability requirements have not been established for water tunnels as they have been for wind tunnels (Reference 1) the acceptability of this repeatability margin could not be determined. Analysis of balance characteristics indicates that the greatest factor affecting repeatability is likely to be the low balance loads encountered in water tunnel testing. Typical individual and combined balance loading for a pitch pause run are presented in Figure 5. The maximum combined load, 0.2 lbs. represents less than 1% of the reported balance force load limits of 25 lbs for forces and 100 in-lbs for moments.

### **FORCE AND MOMENT RESULTS**

Force and Moment comparisons were made with available NASA wind tunnel test data. Select comparisons for longitudinal and lateral-directional coefficients are presented in Figures 6 and 7 respectively. The comparison data is from a test in the NASA Langley 14x22 Tunnel, which was conducted with a full-scale model of the AirSTAR GTM flight test vehicle.

### **FORCED OSCILLATION TESTING**

The oscillatory data comprised a majority of the FVWT Test 006 data. Overall, 159 oscillatory runs were completed. Data reduction procedures to compute dynamic derivatives via two different methods are presented in the following sections. Data were reduced using purpose-written MATLAB scripts and MATLAB release 2013 with no additional toolboxes or analysis packages required. The data reduction methods were based on methods presented in Reference 2.

#### **“SINGLE POINT” METHOD**

The Single Point Method (SPM) calculated dynamic derivatives by curve fitting selected points of the select coefficient data vs. non-dimensional oscillatory rate.

The SPM process for calculating dynamic derivatives is presented graphically in Figure 8. Rolling moment is used in this example though the method applies to pitching and yawing motion as well.

The SPM process consisted of the following steps:

1. ‘Detrend’ the data to remove any balance drift that occurred during the run. This is done by fitting a 2<sup>nd</sup> order polynomial to the moment coefficient vs. time to determine the amount of drift over time. The drift will be subtracted out in step 4 prior to curve fitting.

2. Collect AOA, sideslip, and angular rate values at points corresponding to static conditions within a user-specified angular rate tolerance (denoted by red circles in Figure 8). In the example presented the angular acceleration tolerance was  $0 \pm 0.01 \text{ deg/sec}^2$ .
3. Smooth the moment coefficient using an 11-sample centered moving average. A study was conducted to find an acceptable sample size that smoothed the data without removing the peak values. 11 samples, corresponding to 0.25s at the 40 Hz data rate, was selected.
4. The dynamic derivative,  $C_{lp}$  in the example, is determined by linearly curve fitting the selected points of the moment coefficient moment, less the balance drift determined in step 1, with respect to non-dimensional rate,  $\hat{p}$  in the example. The second axis in Figure 8 shows the selected points, in red, and the linear curve-fit, red line. The slope of the curve fit is the dynamic derivative in question. In this example,  $C_{lp} = -0.162$ .

This process is repeated for each moment coefficient for each oscillatory run. The script calculates  $C_{lx}$ ,  $C_{mx}$  and  $C_{nx}$ ; where 'x' is the oscillatory axis p, q, or r.

### “INTEGRATION” METHOD

The integration data reduction method was used to calculate dynamic derivative coefficients by fitting a Fourier series to the moment coefficient with respect to time. The integration method is presented graphically for a roll oscillation in Figure 9.

The integration method consisted of the following steps:

1. ‘Detrend’ the data to remove any balance drift that occurred during the run. This is done by fitting a 2<sup>nd</sup> order polynomial to the moment coefficient vs. time to determine the amount of drift over time. The drift will be subtracted out in step 4 prior to curve fitting.
2. Filter the moment coefficient. All results presented in this section used an 11 sample centered moving average. A study was conducted to determine the best smoothing span and 11 samples, corresponding to about 0.25 sec at the 40 Hz. data rate, resulted in smoother data without unacceptable loss of peak values.
3. Fit a first-order Fourier series to the data. The dynamic coefficient ( $C_{lp}$  in the example presented) is then determined from the fit according to Equation 1.  $C_{lp}$  for the example presented in Figure 9 is -0.177.

$$C_{lp} = \frac{A_1}{k * Amplitude}$$

Where:

**A1= Fourier Coefficient**

**k = Strouhal Number**

**Amplitude = Amplitude (deg.)**

Equation 1

### EFFECT OF BALANCE DRIFT ON OSCILLATORY DATA

An example of balance drift during a roll oscillatory run is presented in Figure 10. The first axis shows the results of fitting yawing moment with a 1<sup>st</sup> order Fourier fit without detrending the



data. The fit models the lower frequency balance drift rather than the oscillatory motion resulting in inaccurate dynamic derivatives. A solution to the problem of balance drift is to first fit the coefficient time history with a linear or second order polynomial to quantify the balance drift. The second axis in Figure 10 shows the resultant 2<sup>nd</sup> order polynomial fit. Finally, the dynamic derivative can be calculated by fitting the de-trended time history of the coefficient data. The bottom axis in Figure 10 shows the results of fitting the de-trended time history.

## **METHOD COMPARISON VS NASA GTM WIND TUNNEL DYNAMIC DERIVATIVE DATA**

The Single Point Method has advantages and disadvantages compared with the Integration Method. SPM is easily understood. It is easy to apply, requiring only a linear curve fit, and it is more robust with respect to balance drift during the run. The main disadvantage is that it results in larger confidence intervals and uses only a small portion of the collected data. The Integration Method, in comparison, has smaller confidence intervals but is susceptible to balance drift. Figures 11 through 13 show a comparison of the Single Point and Integration data reduction methods vs. NASA GTM wind tunnel data for roll, pitch and yaw oscillations, respectively. The vertical bars on each FVWT data point show the 95% confidence interval for the fit values for each method.

Roll oscillation results, Figure 11, exhibited close agreement between the two data reduction methods and generally good trends between the FVWT water tunnel data and NASA GTM wind tunnel data. The vertical lines represent 95% confidence intervals for the fits involved with the data reduction. The Integration method yields generally smaller confidence intervals by using more of the data for the run. The  $Cl_p$  data trends match the NASA wind tunnel data.  $Cn_p$  matches the NASA data well up to approximately 15 degrees AOA. This trend is repeated with other roll oscillatory series.

Pitch oscillation results, Figure 12, show very good agreement between data reduction methods with the Integration Method having a smaller confidence interval. The  $Cm_q$  data also match the trends from the NASA wind tunnel data closely with a near constant offset throughout the angle of attack range tested.

Yaw oscillation results, Figure 13, show good agreement with NASA data. As with other axes, the Integration method yielded much tighter confidence intervals than the Single Point Method.

## **DYNAMIC MODELING**

### **FREQUENCY-DOMAIN REPRESENTATION OF FORCED-OSCILLATION DATA**

Equivalent system transfer functions were fit to constant-amplitude varying-frequency sweeps in all three axes. Data were reduced using the SIDPAC collection of MATLAB scripts and the methods presented in Reference 3.

The equivalent system fit process consisted of the following steps:

1. Filter output (moment coefficient) data from sweep time history. All data in this section were filtered using a low-pass Butterworth filter to smooth the noise.
2. Remove zero-offset. The mean of the smoothed output data (smoothed moment coefficient) was subtracted from the smoothed output data to reduce any offset about zero. Note that this method did not eliminate balance drift.
3. Time-shift or trim input and output data such that output = 0 at time = 0.
4. Convert input and output signals to frequency domain (SIDPAC 'fint') and fit to transfer function (SIDPAC 'fdoe')

The method for estimating the transfer function was generally successful where the noise was low and there was no balance drift. Roll, pitch, and yaw results are shown in Figures 14 through 16 respectively. A typical pitch sweep is shown in Figure 15 with the preconditioning steps before transforming into the frequency domain. Note that the maximum input frequency was 0.96 rad/sec with the frequency content falling off rapidly above that point. It is expected that a constant rate, varying amplitude sweep would likely have better frequency content and should result in a better transfer function fit. A second-order transfer function typically yielded the best results, with a better match at higher frequencies where the model generated higher loads.

### **Data Reduction Problems**

Less-than-satisfactory results were obtained when FVWT output data were questionable or of poor quality. The data reduction process with noisy and uncorrected moment coefficient data is presented in Figure 17. The noise in the original rolling moment data in the example presented is not sufficiently filtered which results in flat spots at the positive and negative peaks. The drift in the rolling moment signal can be seen as a peak of 0.7 at less than 0.1 rad/sec. The dominant peak in the data is the drift. The resulting estimated transfer function does not match the input data for any reasonable order of equivalent system fit.

### **HYSTERESIS MODELING**

Large-amplitude low-rate pitch and yaw sweeps and bi-directional pitch-pause runs were conducted in an attempt to characterize aerodynamic hysteresis in the GTM model under test. It was expected that hysteresis, if observed, would exhibit characteristics similar to those observed during X-48B flight testing (Figure 18). The characteristics noted, however, were not indicative of hysteresis, instead indicating model or balance issues. Pitch-pause and sweep results for a range of initial AOAs are presented in Figure 19. In the case of sweeps, AOA increasing is denoted by the green traces and AOA decreasing by red traces. A single sweep consists of increasing AOA to the predefined limit then decreasing AOA back to the initial condition. The sweep followed a 1-cos() shape to reduce transients during direction changes. In all low-rate large-amplitude sweep tests and bi-directional sweep tests the moments measured at the balance did not return to their initial values when the model was returned to its initial condition. This resulted in the characteristic loop shape seen in Figure 19. The cause of these shapes was not determined; however, the shapes are somewhat representative of freeplay in the model mounting

system and/or possibly migration of bubbles in the model. After each immersion in the FVWT the model was placed in a series of attitudes to allow bubbles to escape; however, their presence cannot be ruled out completely due to these data artifacts. It must also be noted that shortly after the hysteresis testing the balance failed and became unusable. The effect of intermittent failure or balance degradation prior to failure on the hysteresis sweep data could not be determined.

## **STRIP THEORY MODELING**

Dynamic derivatives were also estimated using strip theory as presented in Reference 4. In this method the contribution of individual model components to dynamic derivatives is estimated based on static (force and moment) characteristics. These contributions can then be summed to form an estimate of six dynamic derivatives. In this evaluation component contributions were based on (in descending order of priority): NASA static data, FVWT static data, and vortex-lattice methods. If component characteristics were not available from a particular source, the next-lowest priority source data were used. Results for three primary damping terms (roll, pitch, and yaw) are presented in Figure 20, and are compared to NASA data and results generated by the vortex lattice tool while developing supplementing static data. Best agreement was achieved in the roll axis which agreed well with NASA data. The other damping terms (pitch and yaw) did not show good agreement but were of similar orders of magnitude. It was noted that the best agreement came from the axis which required the least supplemental data from the linear vortex lattice estimates. It is expected that agreement will improve in the other axes with better static data to use with the strip method. In the interim, however, strip theory provided a reasonable estimation method for first-order estimates of airplane characteristics without the added expense of additional testing to obtain forced-oscillation data.

## **CONCLUSIONS**

### **FORCE AND MOMENT DATA**

Force and moment testing in the BR&T FVWT resulted in mismatches between test data and the test basis. These mismatches can be attributed to balance loading and resolution, differences in scale and Reynolds Number, and the data trended similarly when compared to NASA wind tunnel data. Additional testing to further evaluate balance loading and resolution effects with an improved balance are planned for CY2014.

### **OSCILLATORY DATA**

The FVWT has proven to be a low cost method for obtaining dynamic derivative data compared to flight testing and wind tunnel testing. Roll, pitch and yaw oscillation data was successfully reduced via two different methods using MATLAB based data reduction scripts written to accomplish the task efficiently. The oscillatory data compares favorably with NASA wind tunnel data.

Additional data collection efforts were delayed due to an issue with the water tunnel balance. These tests will be completed when the balance is repaired or replaced.

## **DYNAMIC MODELING**

These tests and analysis demonstrated the frequency domain technique of an equivalent system fit to capture the frequency dependencies of dynamic aerodynamic terms. Also confirmed was the applicability of strip theory for preliminary estimates of airplane dynamic derivatives. Hysteresis modeling efforts were inconclusive due to questionable test results. Additional testing with frequency sweeps designed to increase the frequency content of the resulting moments, and to reevaluate hysteresis characteristics with an improved balance are planned for CY2014.

## **REFERENCES**

1. Barlow, J., Rae, W. H., and Pope, A., Low Speed Wind Tunnel Testing third edition ISBN 9788126525683
2. Vicroy, D.D; Daniel G. Murri, D. G.; and Grafton, S. B., " Low-speed Dynamic Force Tests of a Subsonic Blended-Wing-Body Tri-jet Configuration", NASA/TM—2010–216198,2010
3. Murphy, P. C., Klein, V.: Validation of Methodology for Estimating Aircraft Unsteady Aerodynamic Parameters from Dynamic Wind Tunnel Tests, AIAA Paper 2003-5397, August 2003.
4. Wykes, J. H. et. al; "An Analytical Study of the Dynamics of Spinning Aircraft", WADC Technical Report 58-381, December 1958

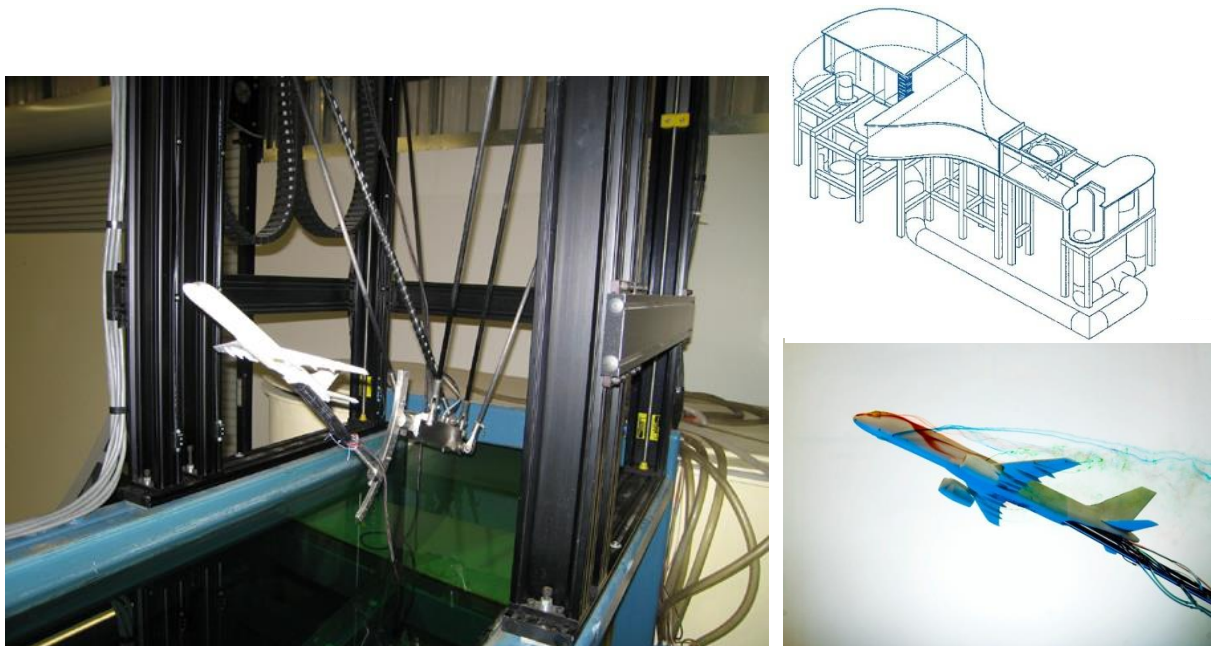


**Figure 1. Boeing's Dynamic FVWT**

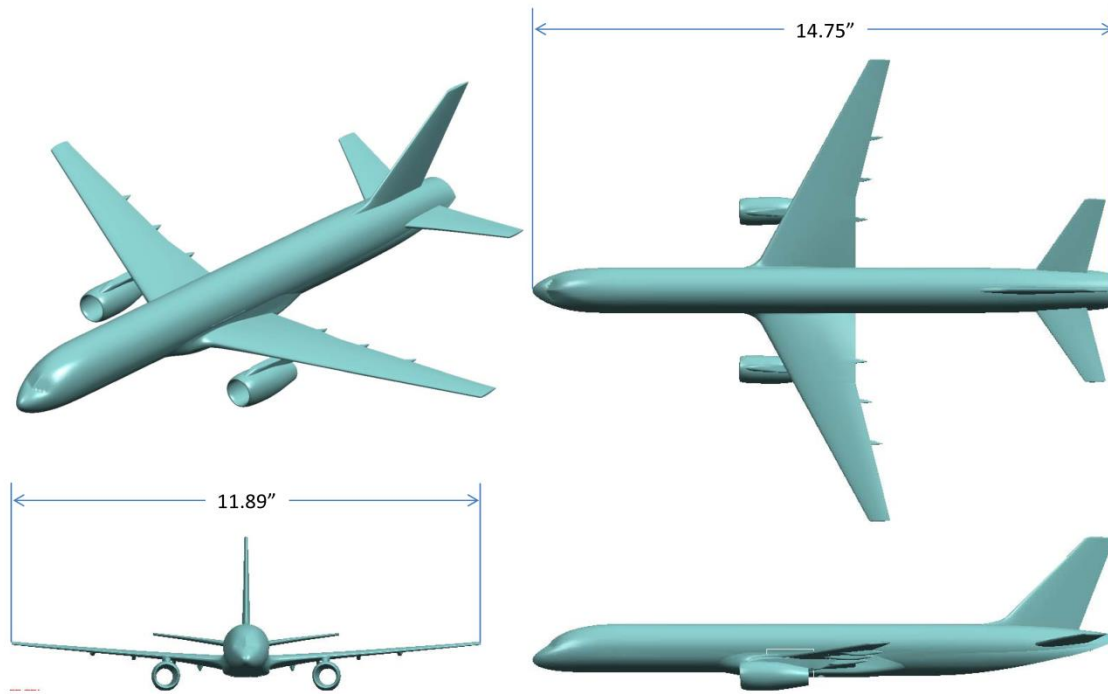


**Figure 2: FVWT Generic Transport Test Model**

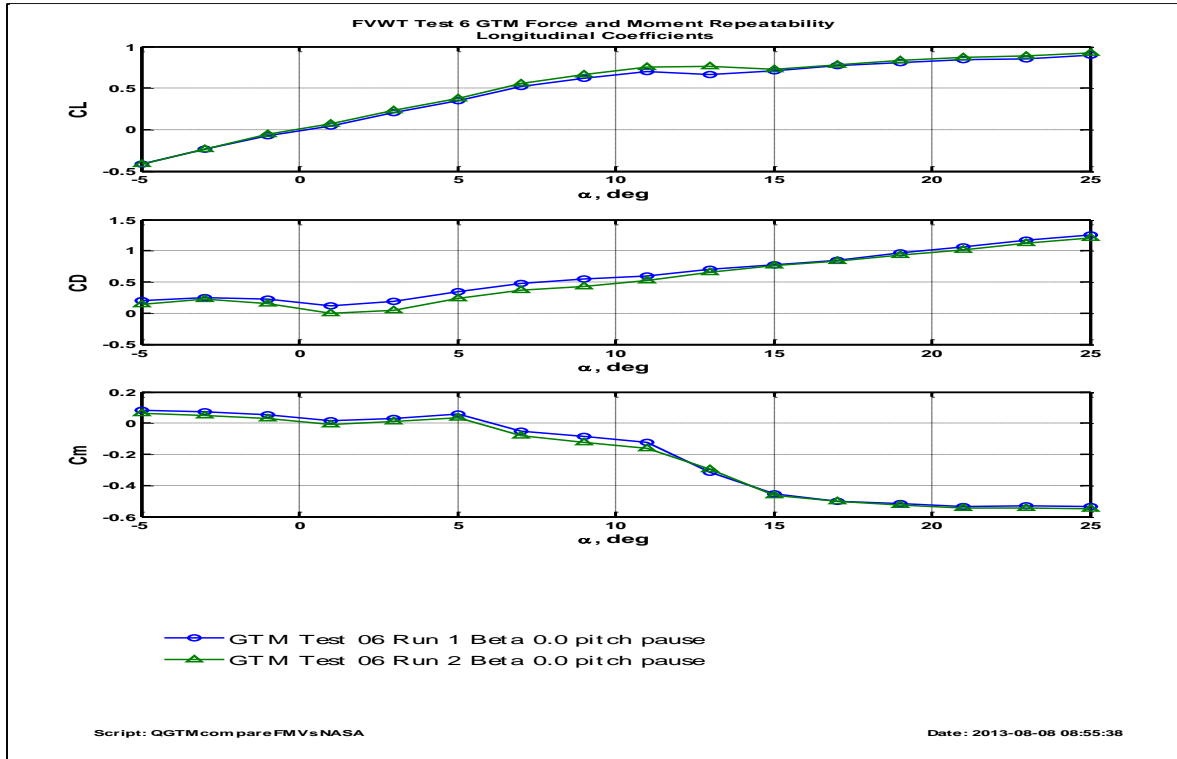


Figure 3: Longitudinal Force and Moment repeatability for back to back repeat runs.

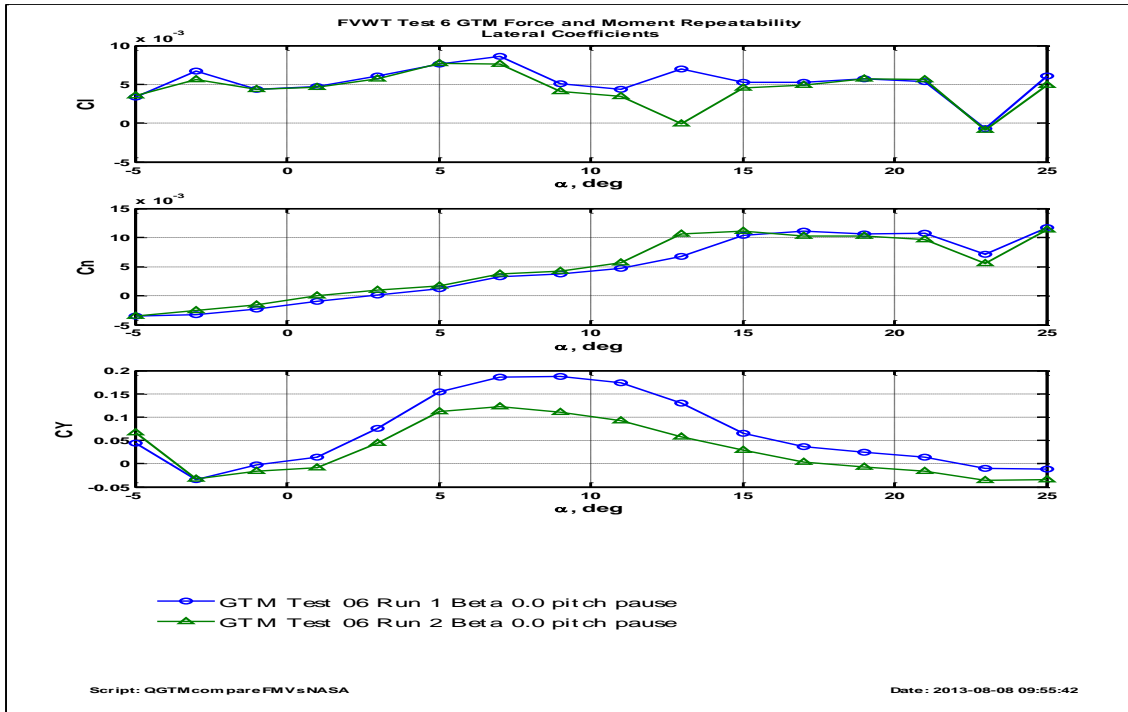
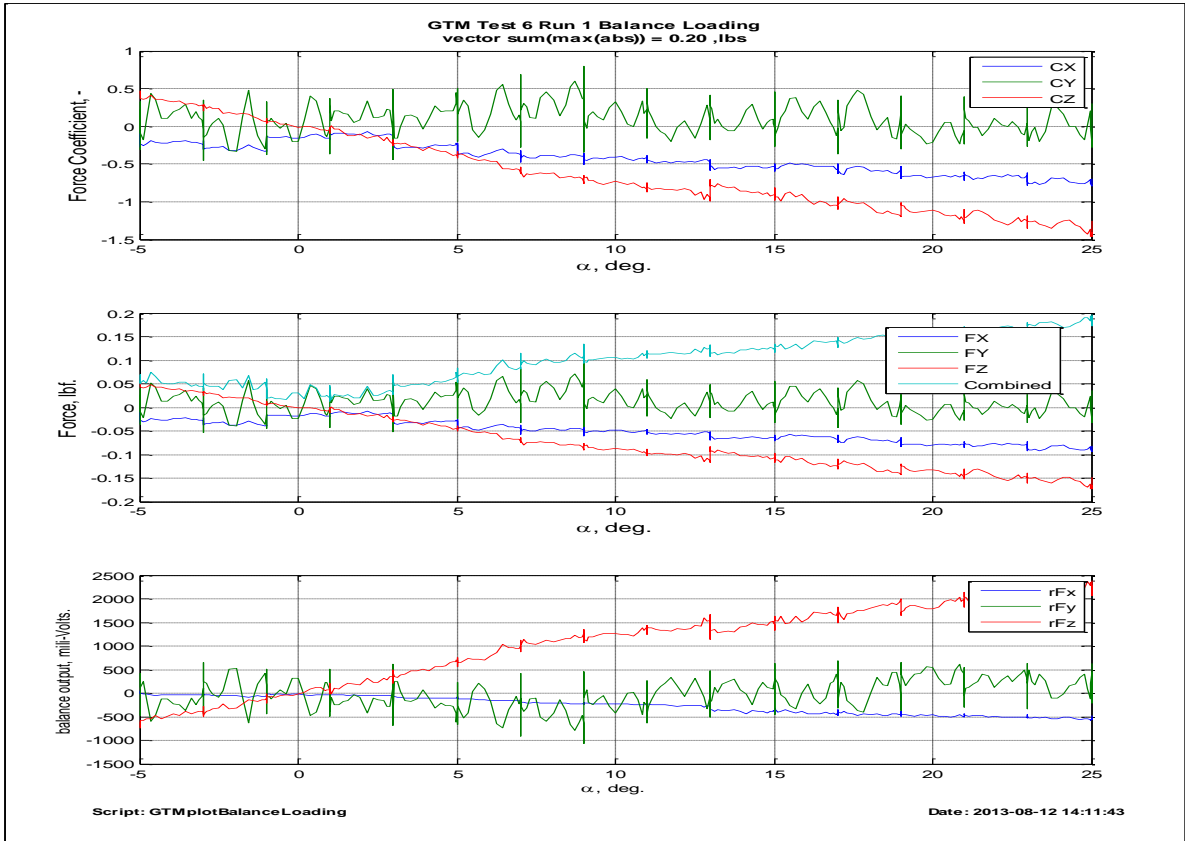


Figure 4: Lateral Force and Moment repeatability for back to back repeat runs



**Figure 5: Typical Balance Loading for a Pitch-Pause Run**

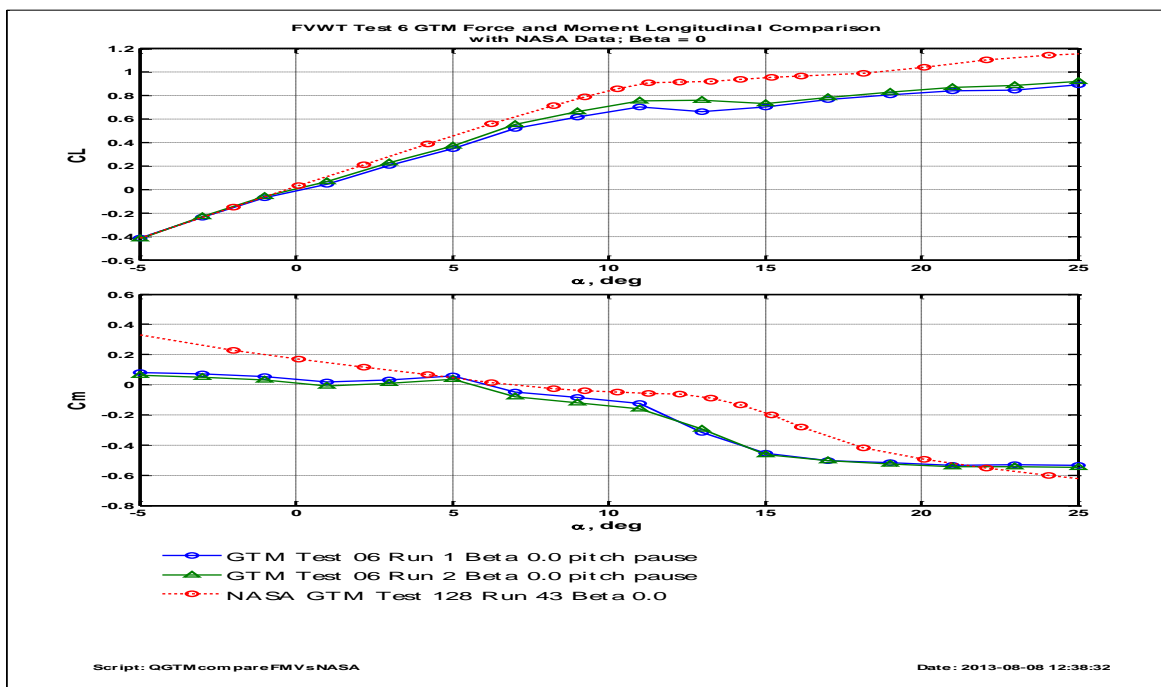


Figure 6: Longitudinal Comparison with NASA Wind Tunnel Data

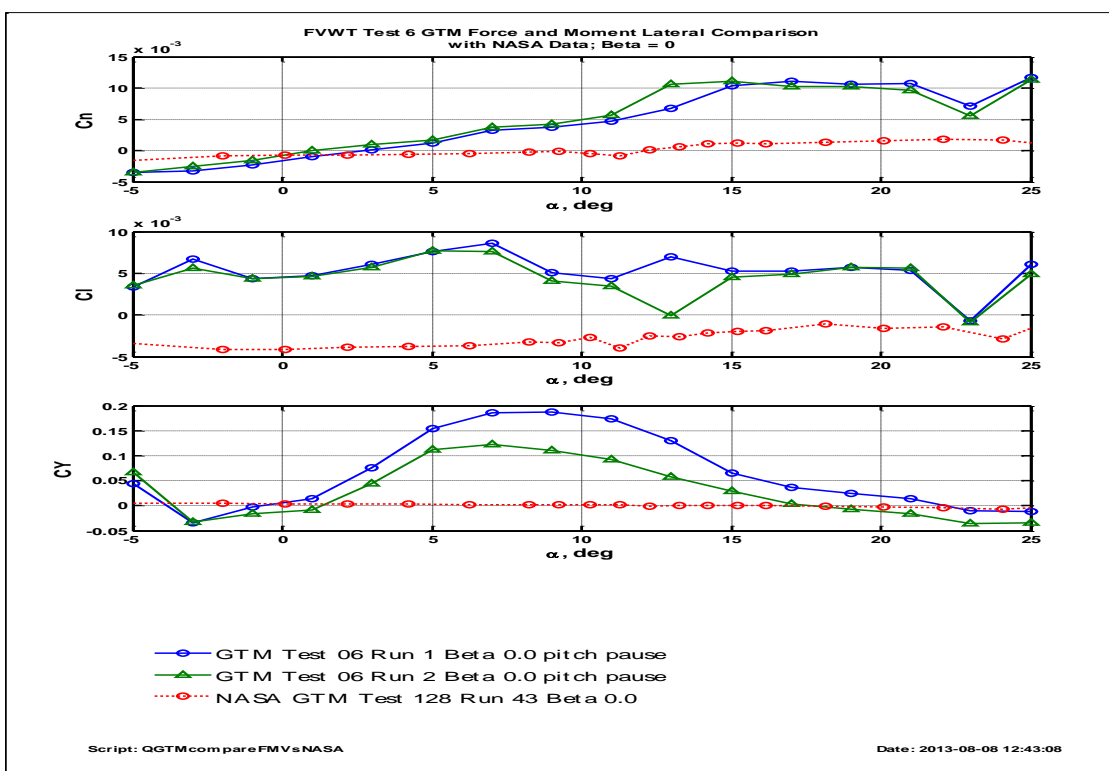


Figure 7: Lateral Comparison with NASA Wind Tunnel Data



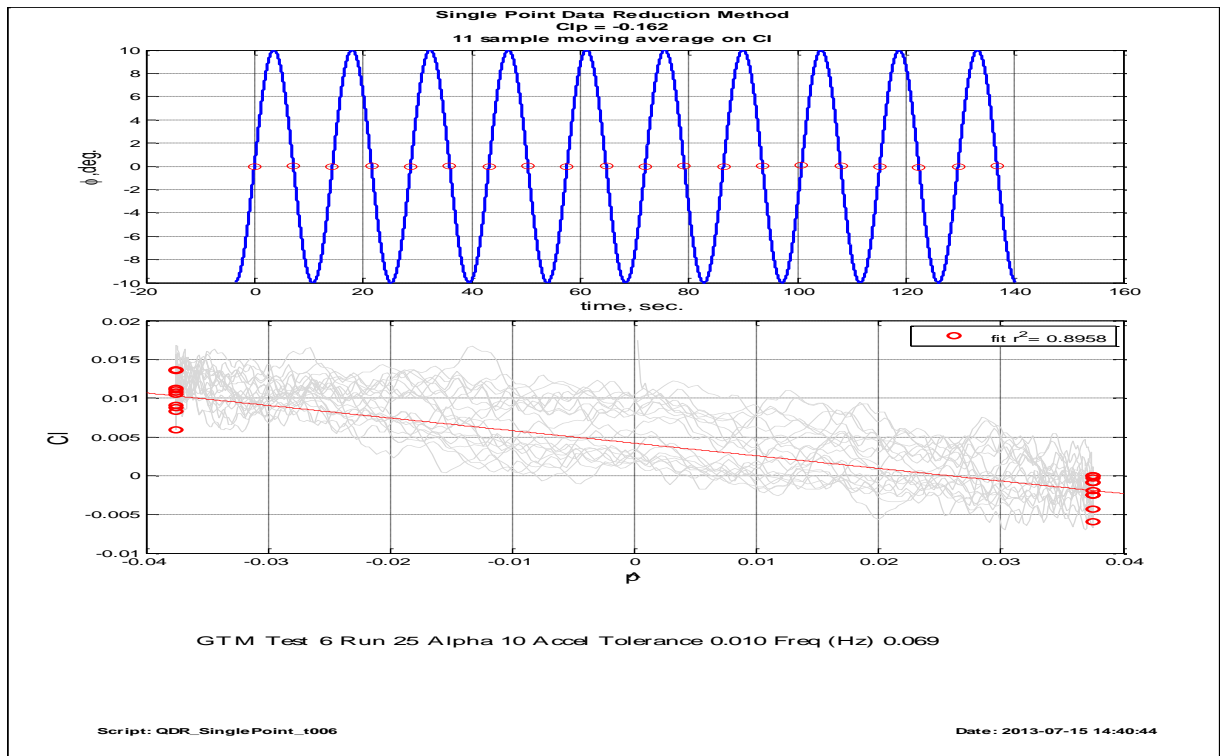


Figure 8: Example Clp calculation using the single point method.

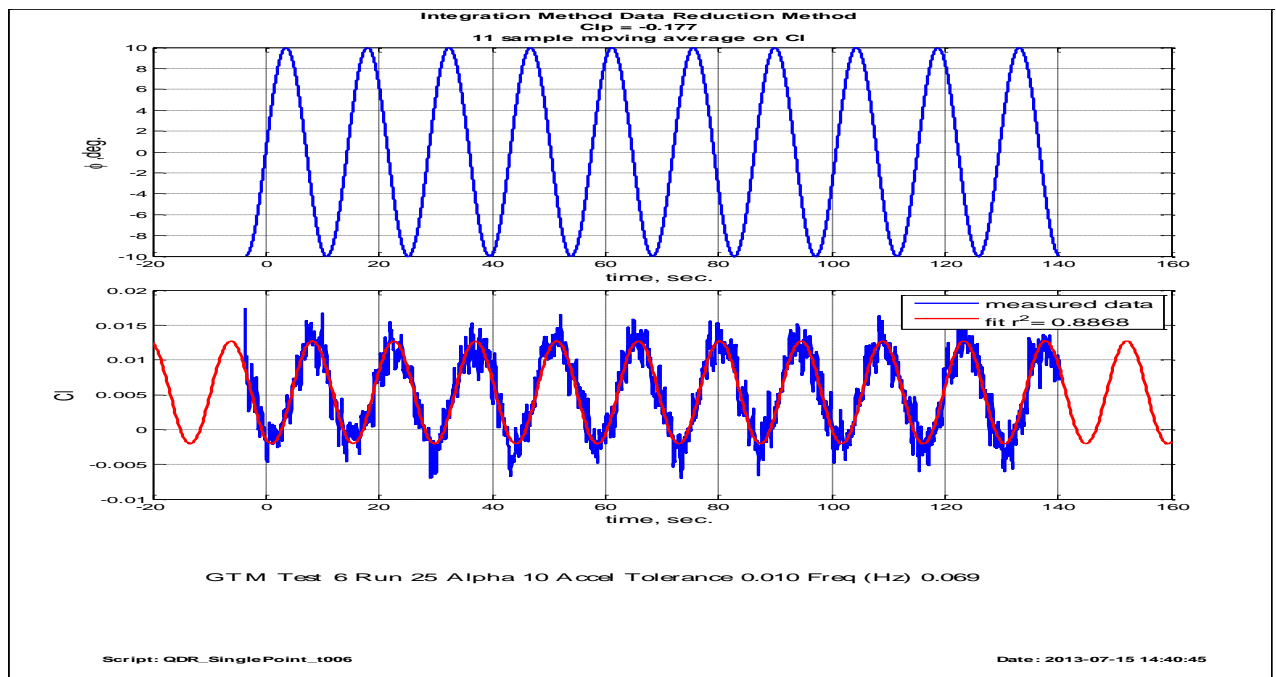


Figure 9: Example Clp calculation using the integration method.

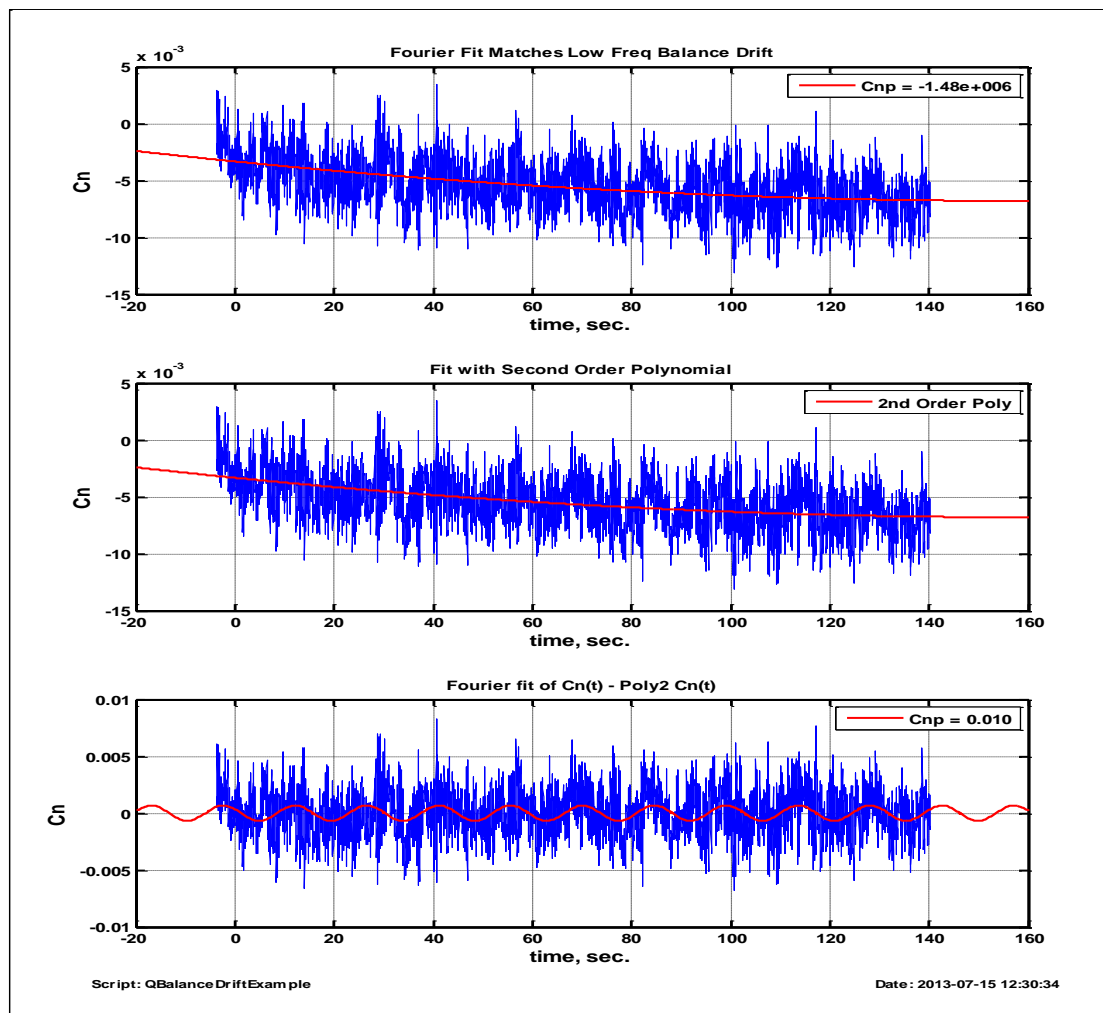


Figure 10: Yaw axis balance drift during rolling oscillatory motion.

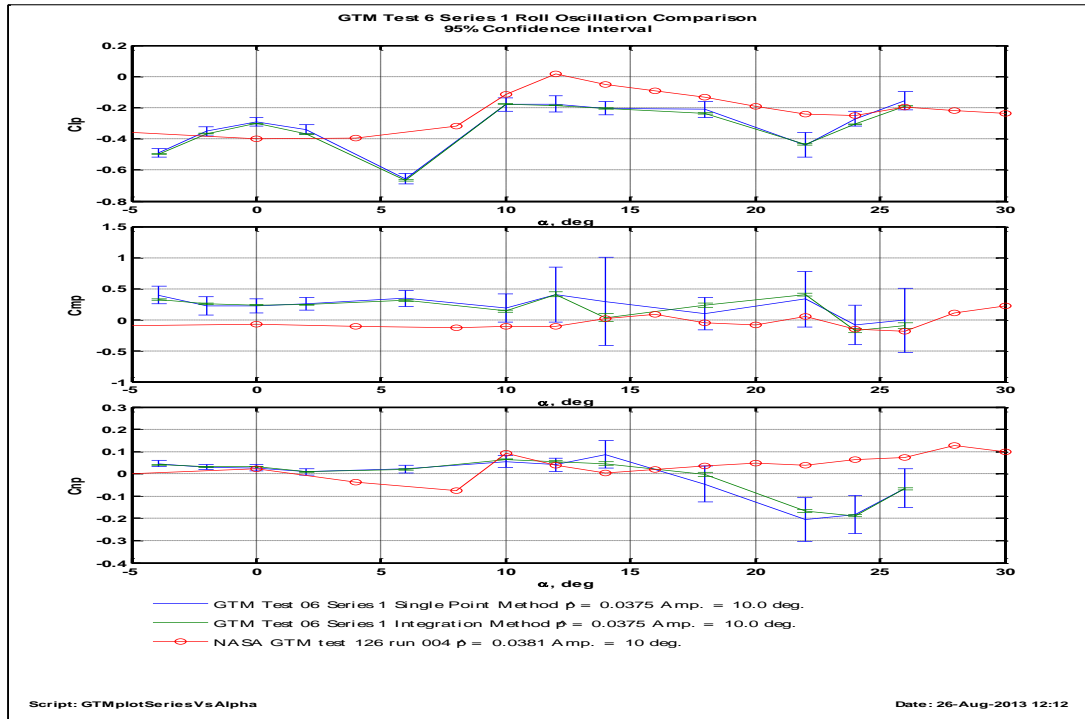


Figure 11: Comparison of the Single Point and Integration Data Reduction Methods vs NASA GTM wind tunnel data for a roll oscillatory series.

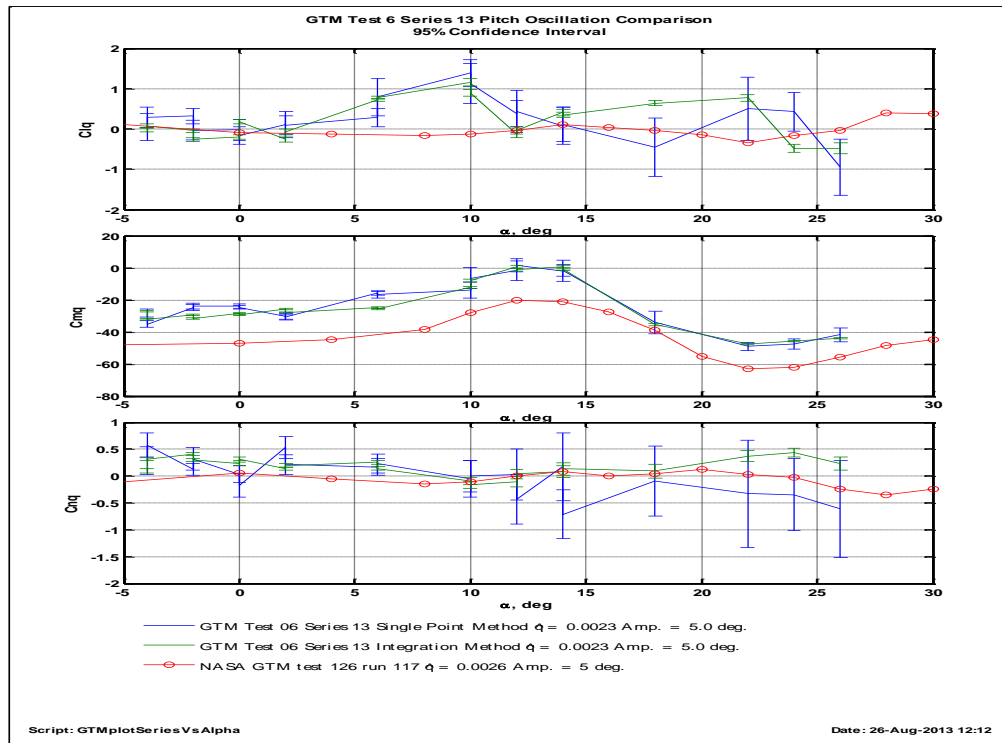
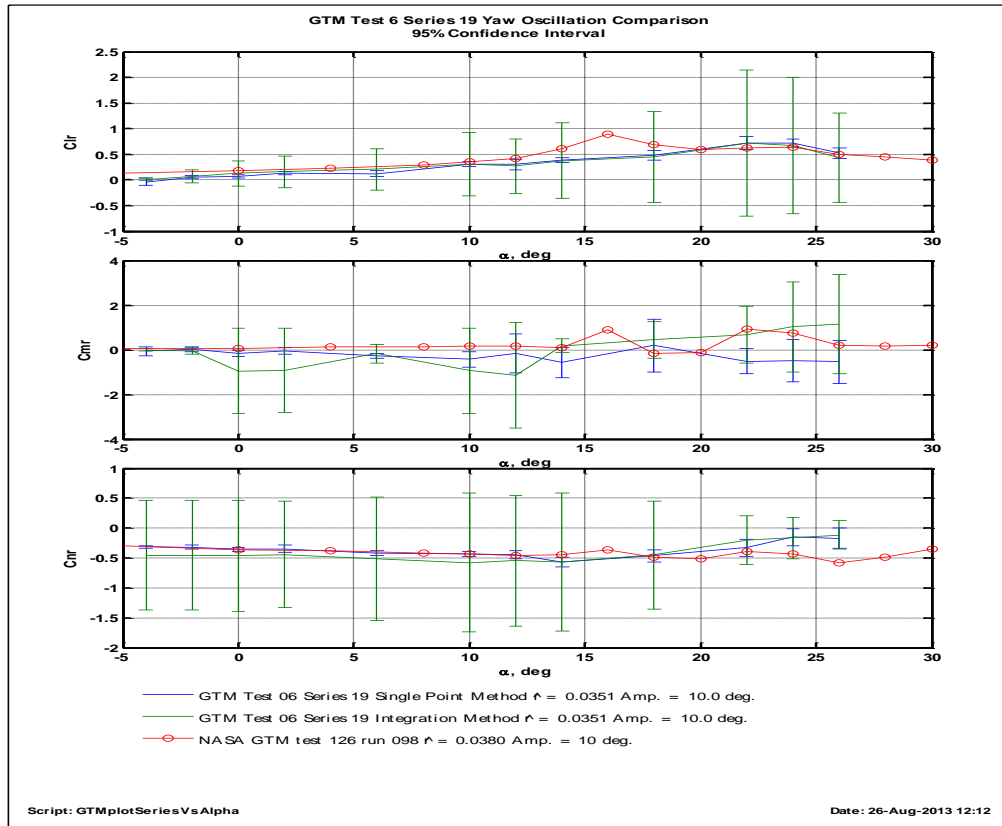


Figure 12: Comparison of the Single Point and Integration Data Reduction Methods vs NASA GTM wind tunnel data for a pitch oscillatory series.



**Figure 13: Comparison of the Single Point and Integration Data Reduction Methods vs NASA GTM wind tunnel data for a yaw oscillatory series.**

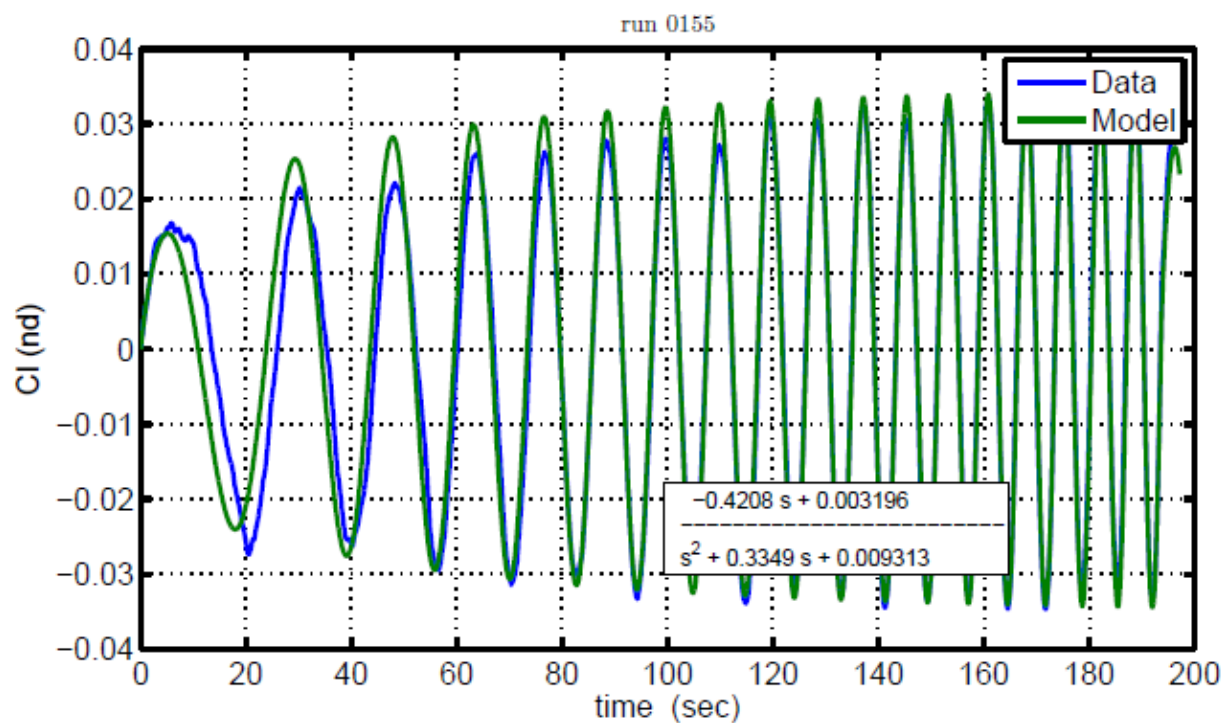
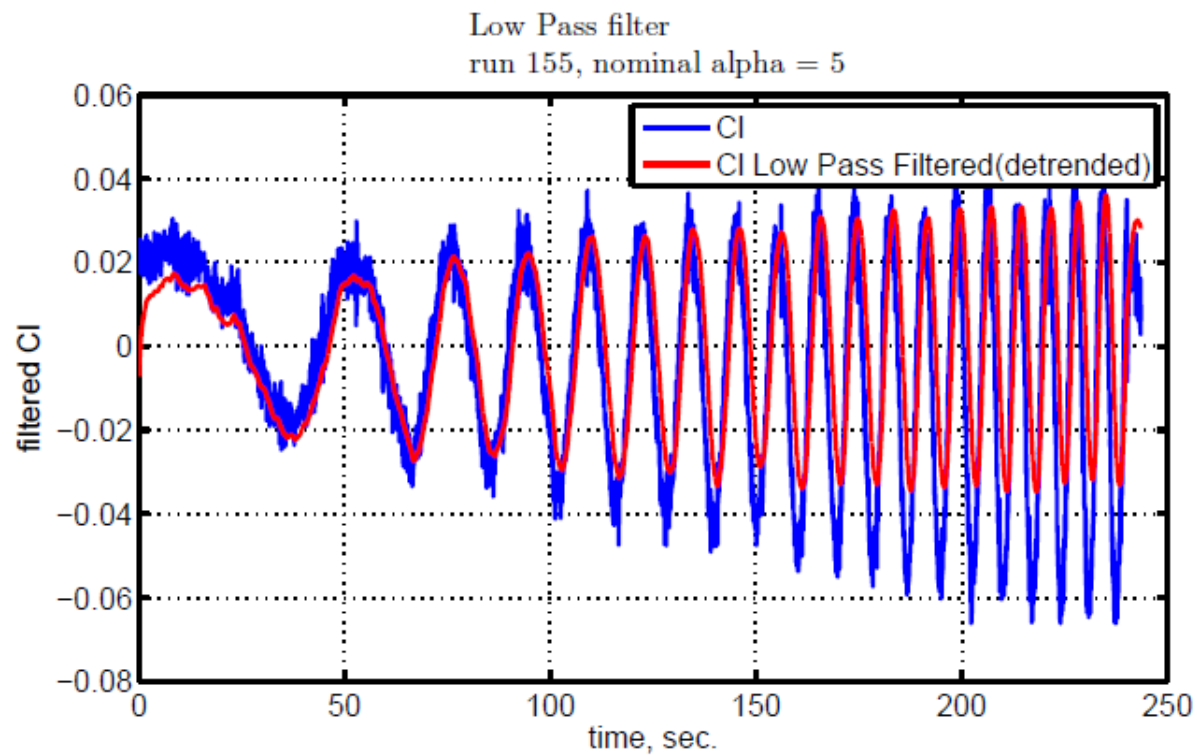


Figure 14: Frequency Domain Transfer Function Fit, Roll Rate Sweep.

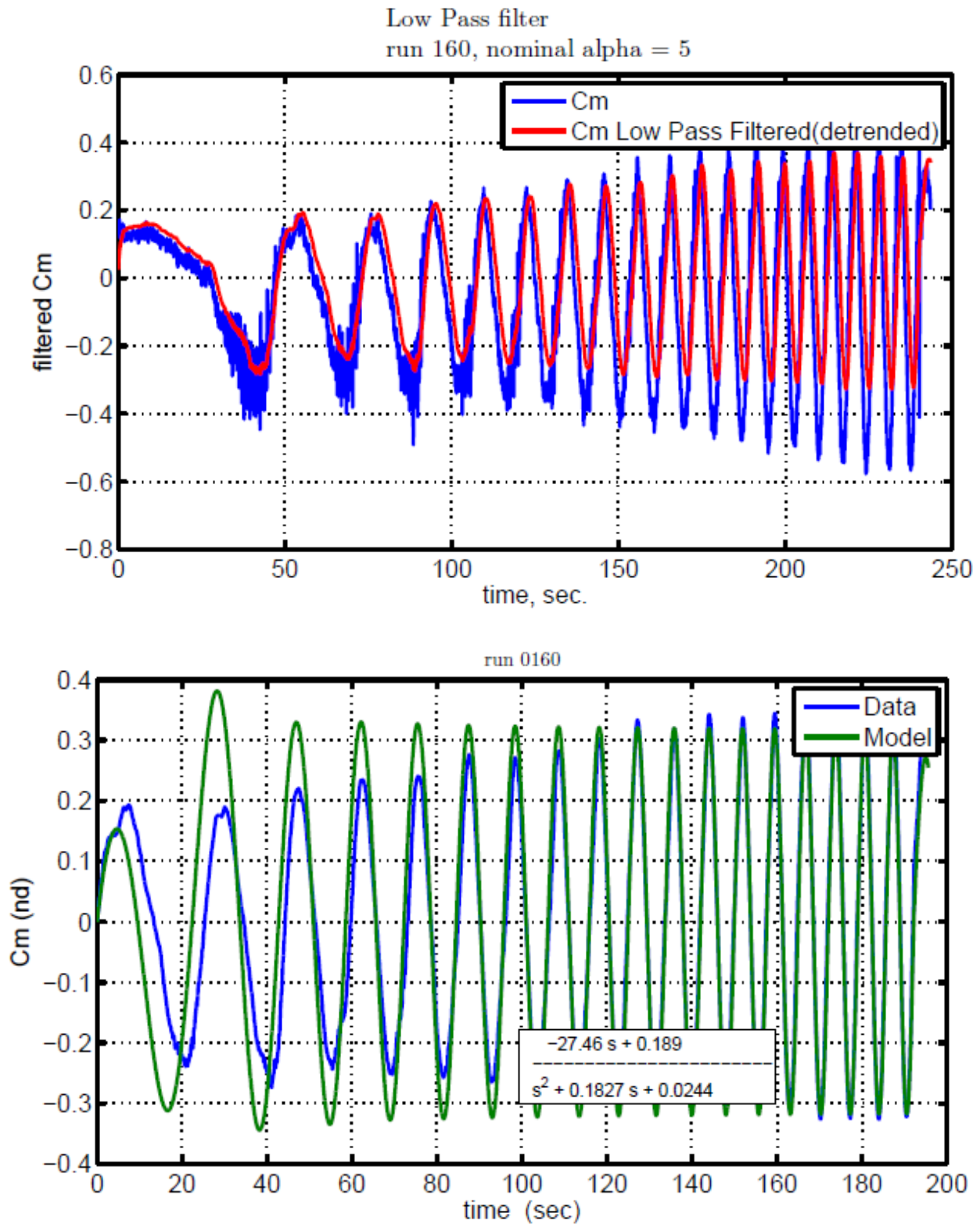


Figure 15: Frequency Domain Transfer Function Fit, Pitch Rate Sweep.

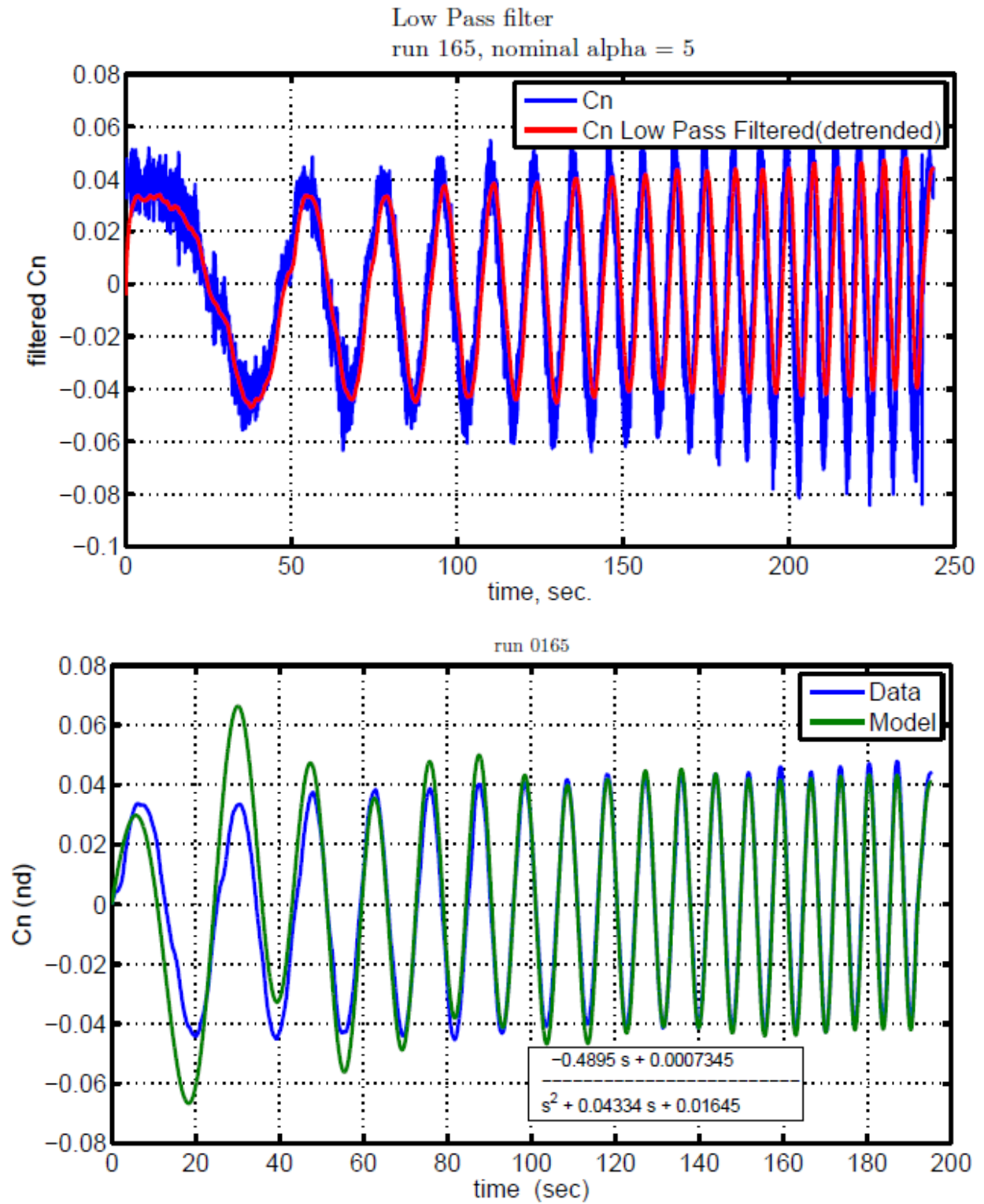


Figure 16: Frequency Domain Transfer Function Fit, Yaw Rate Sweep.

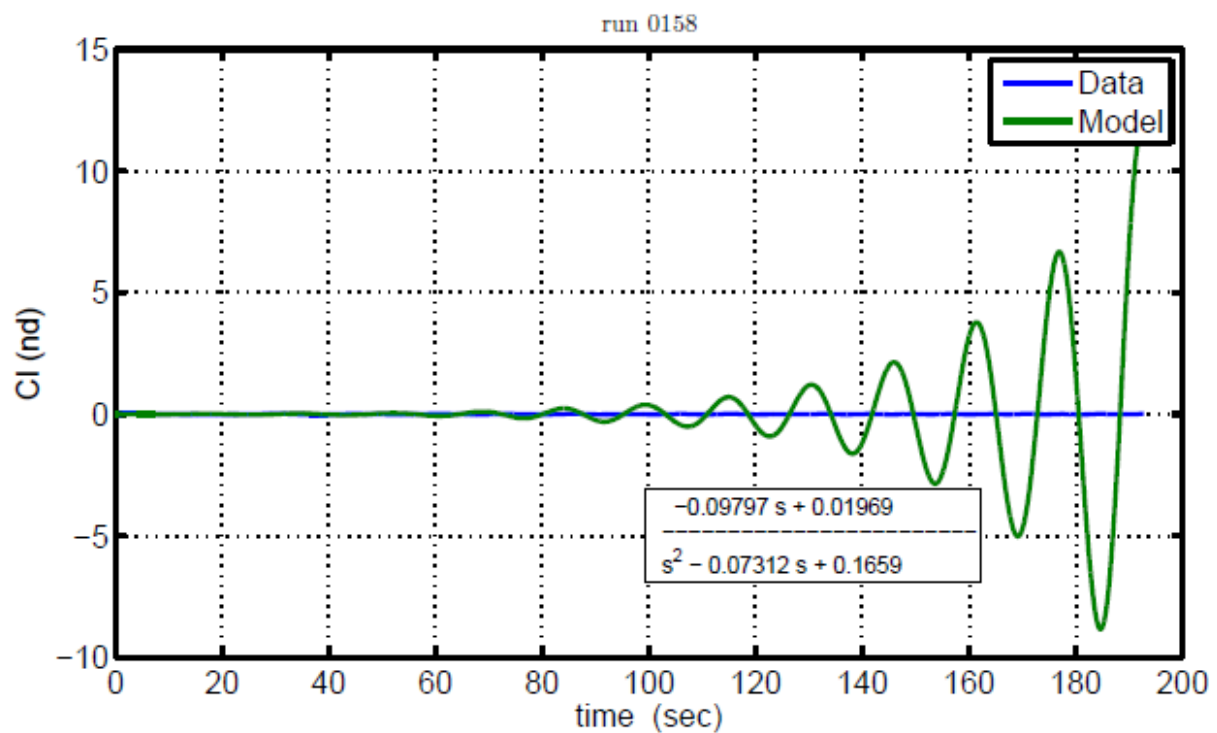
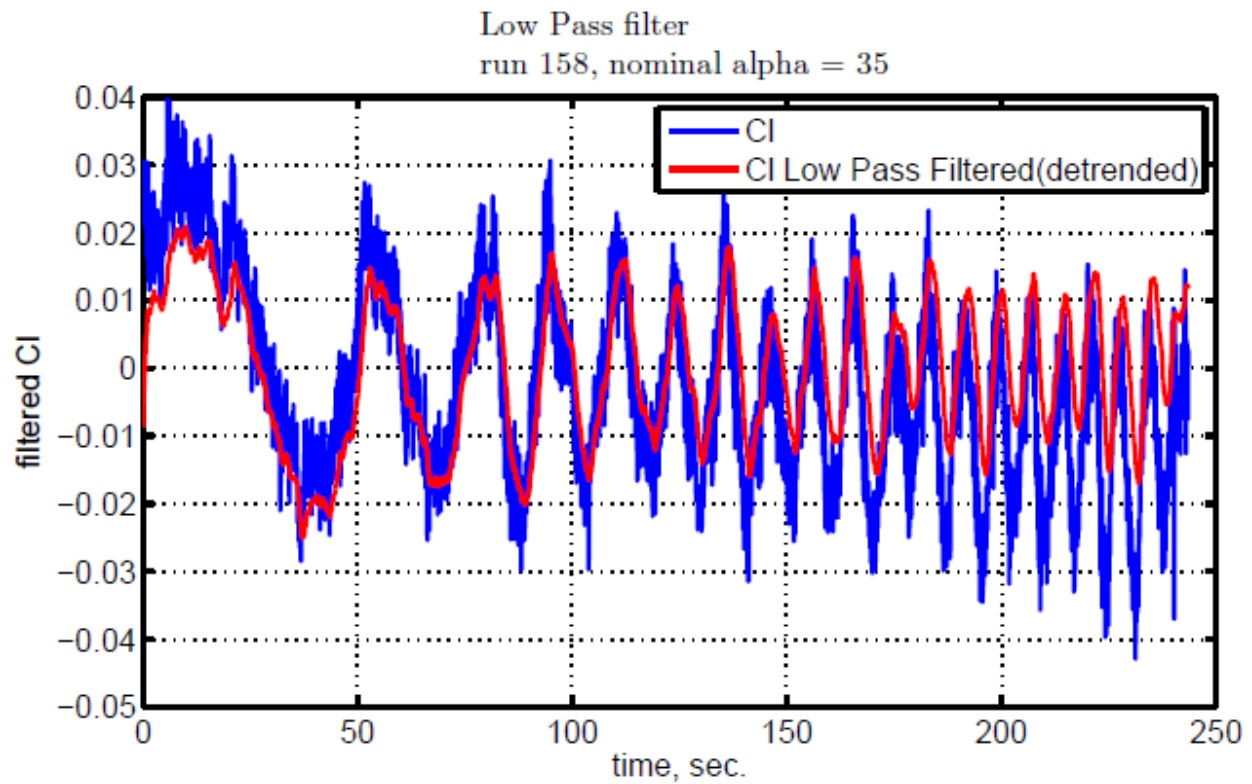


Figure 17: Example of Bad Frequency Domain Transfer Function Fit Due to Degraded Moment Signal, Roll Rate Sweep.



### Example Data from X-48B Flight Test

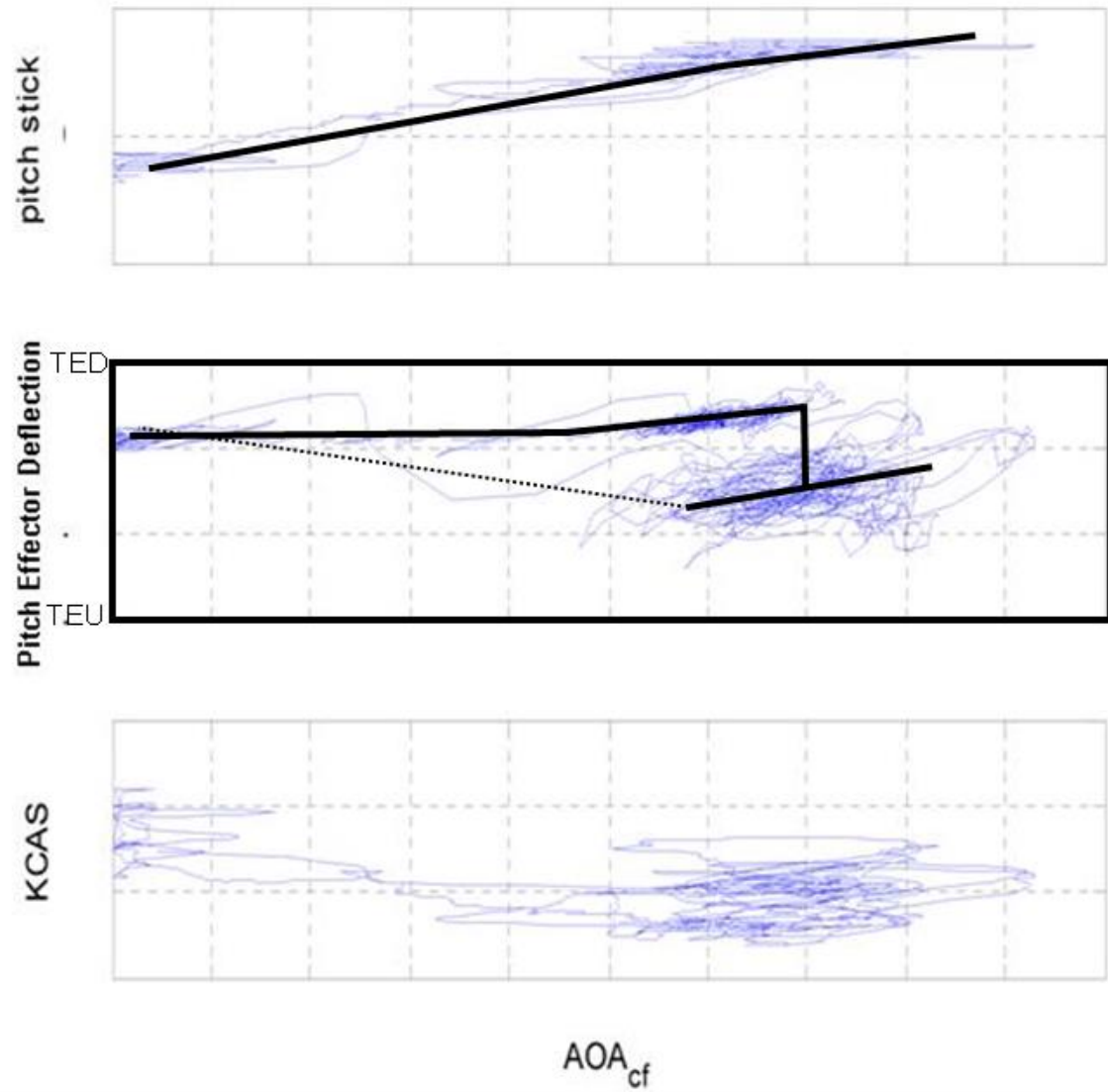


Figure 18: X-48B Aerodynamic Hysteresis Example.

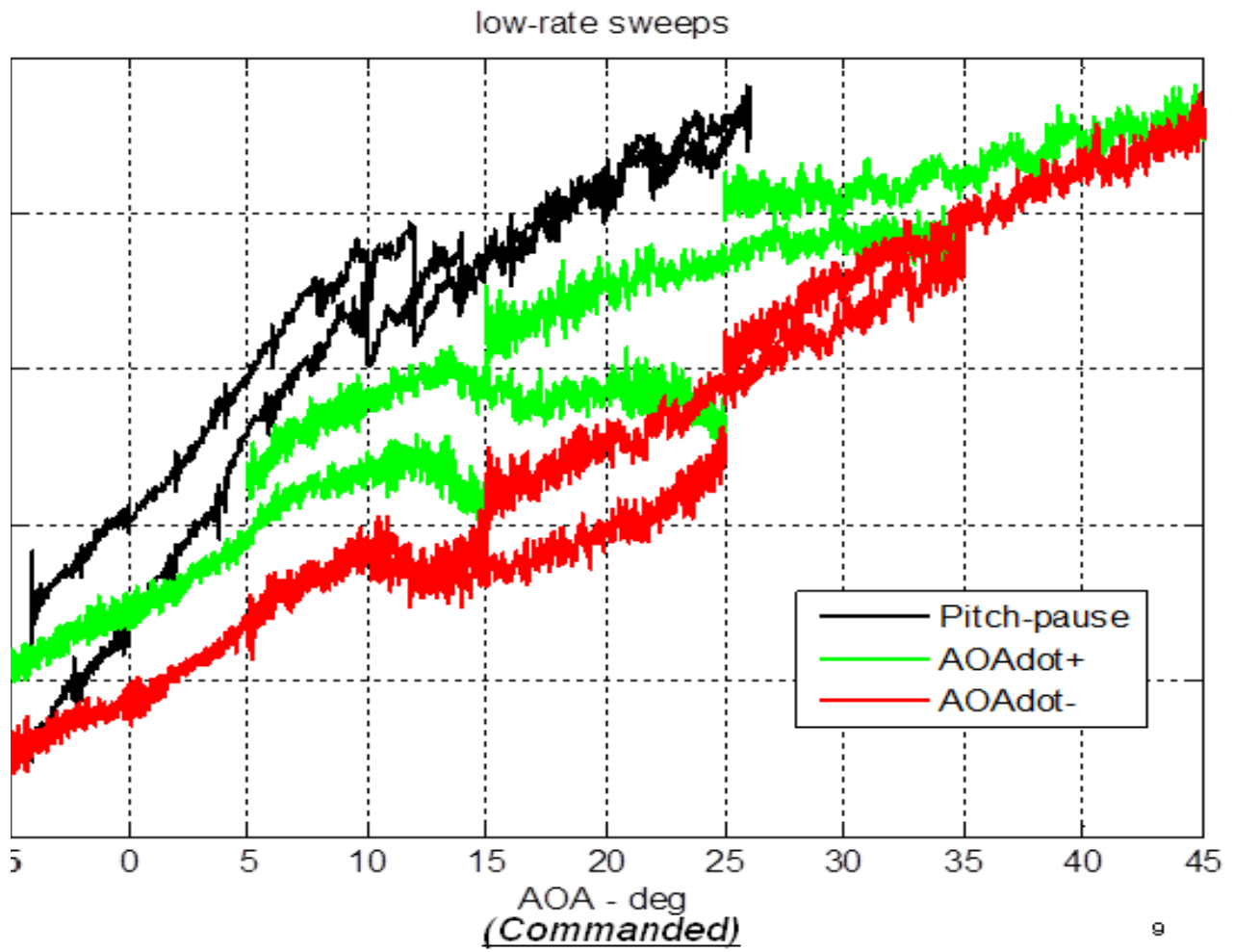


Figure 19: GTM/FVWT Hysteresis Investigation Result.

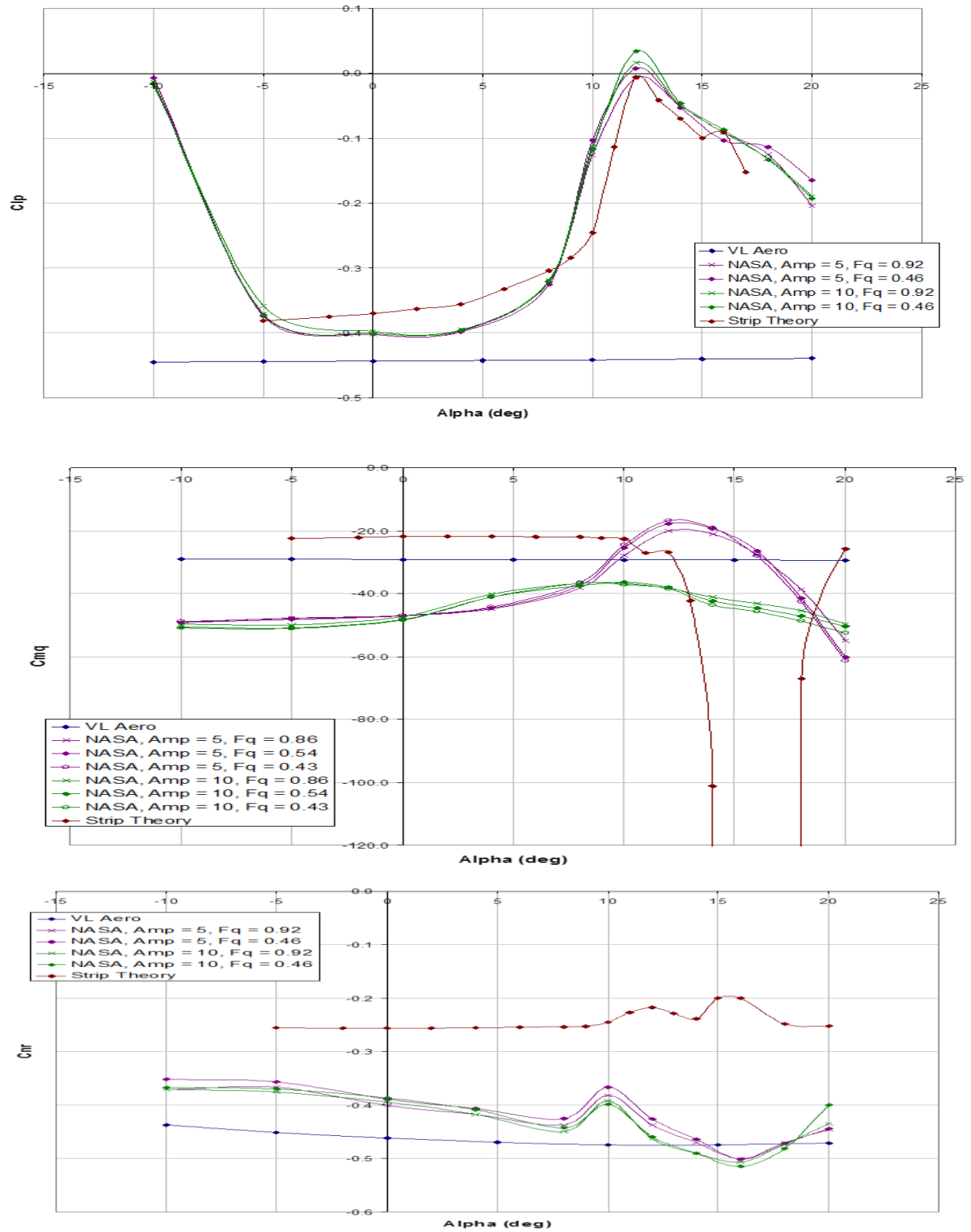


Figure 20: GTM Strip Theory Results Comparison.